Mutual Inductance Calculation Between Arbitrarily Positioned Polygonal Coils

ZHANG Zijian[1], *SHAO Ming*[1,2], *SHANG Kai*[3], *LI Xuekong*[4], *HUANG Chunliang*[4], *SHI Jinku*[4], *CUI Huaxian*[4], *DONG Yangyang*[1*]

1. College of Astronautics, Nanjing University of Aeronautics and Astronautics, Nanjing 210016, P.R.China;
2. The 804th Research Institute of Shanghai Aerospace Technology Research Institute, Shanghai 201100, P.R.China;
3. The 41st Research Institute of CASIC, Huhhot 010010, P.R.China;
4. Huaneng Guangxi Clean Energy Co., Ltd., Nanning 530028, P.R.China

(Received 15 April 2022; revised 20 June 2022; accepted 10 July 2022)

Abstract: Polygonal coil systems are designed for increasing and more kinds of sensors and electromagnetic systems. This paper presents a method for calculating mutual inductance between polygonal coils including irregular polygons. Based on the Biot-Savart law, the method calculates mutual inductance by dividing a polygonal coil into finite wires, and expresses the magnetic induction intensity generated by the excitation coil as a function of the spatial position of each vertex of the coil. The calculation method of the feasible region of the objective function is updated and the calculation process is simplified, so the calculation accuracy is improved. For octagon coils arbitrarily positioned in space, the accuracy of the algorithm is verified by the simulation and experiment.

Key words: mutual inductance; polygonal coils; Biot-Savart law; arbitrary position

CLC number: TH89 **Document code:** A **Article ID:** 1005-1120(2022)S-0120-07

0 Introduction

To meet the diverse and increasing equipment needs involved in biomedicine and electronic industry, multiple configuration of the sensors is designed. For instance, biomedical equipment, such as long-term implantable devices, need to specifically designed coil configurations to meet the stringent requirements of the use environment. Besides, in the evaluation and optimization of sensor with polygonal coils, such as precision and responsiveness, the accurate inductance calculation can help researcher design the sensors[1-3]. The research of mutual inductance parameter calculation in this paper is valuable and practical.

Mutual inductance is a basic parameter in coil system or sensor field, and its advantages are reflected in many industries. Nowadays, wireless power transmission (WPT) system is in the ascendant in the rapid development of science and technology society. Refs.[4-5] assumed that mutual inductance parameter had effects on MRC-based WPT systems and energy efficiency. They exemplified the energy efficiency in WPT system to fulfill various functional requirements according to the changes of mutual inductances among several coils. However, their simulations and experiments are incomplete in that they only to move the primary coil and secondary coil to tune the mutual inductance and ignore the effects on rotation. Refs.[6-7] introduced the electromagnetic-based nondestructive evaluation (NDE) of metallic components. They took the advantage of the inductance between coils to induce the position where the cracks happened. In their experiments, eddy current testing (ECT) method was used to replace the traditional planar induction coil. The planar induction magnetic field sensor can detect cracks on non-magnetic samples. Refs.[8-11]

*Corresponding author, E-mail address: yy.dong@nuaa.edu.cn.

How to cite this article: ZHANG Zijian, SHAO Ming, SHANG Kai, et al. Mutual inductance calculation between arbitrarily positioned polygonal coils[J]. Transactions of Nanjing University of Aeronautics and Astronautics, 2022, 39(S): 120-126.
http://dx.doi.org/10.16356/j.1005-1120.2022.S.016

used the coupling inductance parameter to realize the position in door. Different bandwidth and frequency separation were used to improve the accuracy. The inductive coupling and inductance between the moving coil and several fixed coils were measured separately in room. From this case, mutual inductance calculation between coils arbitrarily positioned is of great meanings. The above case introduces the application scenario of mutual inductance parameters

At present, the calculation of mutual inductance is computed by applying Newman's formula directly which is suitable for a curved coil and using other numerical methods. When it comes to polygonal coils, the algorithm with Biot-Savart law will be simplified and accurate. Refs.[12-13] gave the formula on the calculation of mutual inductance between polygon coils like triangle, square, hexagon, octagon coils in the last century. Ref.[14] suggested the mutual inductance between polygon coils equals to that of circular coils when their area is the same and validated the formula with mathematical tools like series and integrals. However, when the number of sides of a polygon is few, the error rate of the approximate circular coils is hard to neglected. A new solution, 3-D analytical calculations based on green's function (integral approach) is assumed in Ref.[15] to calculate mutual inductances and magnetic force between coils which have rectangular cross sections. Since different coils always need to be considered, this calculation cannot be used as a general solution. Ref.[16] derived the formula on coaxial and parallel circular coils. Their methods have limitations in application scenarios. Ref.[17-18] used the second order vector potential to calculate the mutual inductance of rectangular spiral coil. When it comes to the simplified model, he replaced the rectangular spiral coil to a series of single rectangular coils with rectangular cross-section. In 2017, he gave the calculation of coupling coefficient between two arbitrary-shaped coils with primary coil function and secondary coil complex conjugate.

Refs.[19-20] introduced the formula to calculate mutual inductance between circular filaments arbitrarily with the approach of the magnetic vector potential, which was consistent with Grover's result in Ref.[21]. The posture of the circular coils arbitrarily positioned is deduced by the equation of the plane and the coordinates of the coil center. Slobodan Babic's formula needs to collect all physical parameters of the coils and establishes functional relationship. Instead, this paper simplifies the procedure that the new formula needn't the equation of the plane and the coordinates of the coil center. Refs.[22-23] also used Biot-Savart law to calculate the mutual inductance between coaxial coils. He directly used analysis formula instead of numerical integration to process the integral. Meanwhile, he deduced mutual inductance between two planar spiral coils with an arbitrary number of sides based on the partial inductance method instead of Biot-Savart formula. In fact, Biot-Savart formula is meant to calculate the magnetic induction intensity of straight wire, which also means Biot-Savart formula is suitable for the polygon.

In this paper, we intend to expand the formula which can calculate the mutual inductance to N-polygon coil to meet the needs of the sensor designer. We derive the new arithmetic of mutual inductance when the polygonal coils are arbitrarily positioned. The new analytic methods divide the polygon into several sides to deduce magnetic induction intensity based on Biot-Savart law. The magnetic induction intensity function made up of the coordinates of the vertices is given, suitable for polygonal coils, even irregular coils. Besides, the methods update the computation of the feasible region of the objective function, which simplify the procedure and enhance the accuracy of the calculation. In this paper, we will also use available research data for comparison to validate our formula' accuracy.

1 Modeling of Analysis of Coils

1.1 Functions for magnetic induction intensity

Before the calculation of the mutual inductance, we need to derive the function for magnetic induction intensity (B_{mag}) produced by straight wire, as is shown in Fig.1. The line AD is the ener-

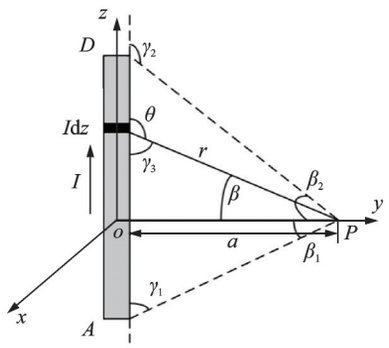

Fig.1 Magnetic induction intensity produced by straight wire

gized straight wire, Idz is current element and point P is any point outside the line AD.

Based on Biot-Savart law, magnetic induction intensity produced by current element (Idz) at point P is

$$dB_{mag}=\frac{\mu_0}{4\pi}\cdot\frac{Idz\sin\theta}{r^2} \tag{1}$$

where μ_0 is the vacuum permeability, a the distance from point P to line AD, r the distance from point P to current element (Idz).

$$z=-a\cot\theta,r=\frac{a}{\sin\theta},dz=\frac{ad\theta}{\sin^2\theta} \tag{2}$$

With geometric relations above and substitute the parameters into equation, we can derive the integral formula on B_{mag}

$$B_{mag}=\frac{\mu_0 I}{4\pi a}\int_{\beta_1}^{\beta_2}\cos\beta d\beta \tag{3}$$

Substitute the parameters into Eq.(2), and the function for magnetic induction intensity is deduced

$$B_{mag}=\frac{\mu_0 I}{4\pi a}(\cos\gamma_1+\cos\gamma_2) \tag{4}$$

where γ_1 and γ_2 are determined by the coordinates of points A, D, P.

Because of the secondary coil, namely the integral area, fixed on plane xoy, the effective value of B_{mag} is the component projected on the z-axis (BF_{mag}) based on the definition of magnetic flux.

$$\boldsymbol{e}=\frac{AD\times DP}{|AD\times DP|},\sin\theta_v=\boldsymbol{e}\cdot\boldsymbol{e}_z \tag{5}$$

$$BF_{mag}=B_{mag}\times\sin\theta_v \tag{6}$$

where $\boldsymbol{e}$ is the unit direction vector of B_{mag}, $\boldsymbol{e}_z$ the unit normal vector of plane xoy, θ_v the angle between B_{mag} and plane xoy.

1.2 Calculation of coordinates of vertices

From the above, we derive the magnetic induction intensity function of the coordinates of straight ware's endpoints, so the endpoints of polygon must be figured out for B_{mag}.

Fix the secondary coil on the plane xoy, where the center of the secondary coil corresponds to the origin o and the center of the primary coil corresponds to the point o'. As shown in Fig.2, the center of the primary coil is the point o' which is arbitrarily positioned in space. In Fig.2, δ is $2\pi/n$, n means the number of sides of a polygon. Fig.3 gives the coordinates of secondary's vertices in plane xoy. In Fig.3, X_1, X_2, X_i, X_n are the vertices of the polygon.

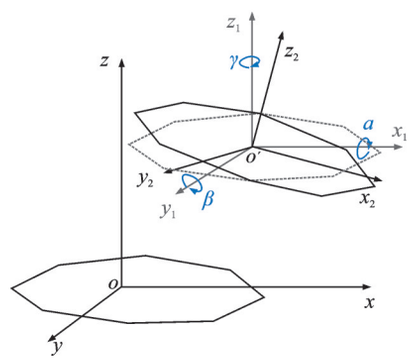

Fig.2 Two n-polygon coils arbitrarily positioned in space

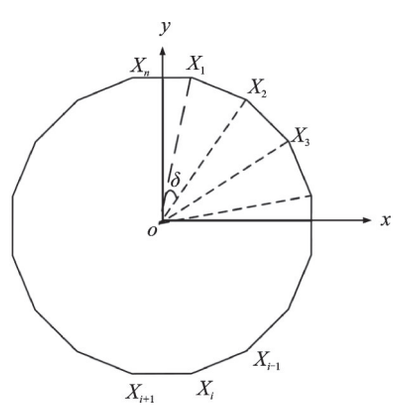

Fig.3 Coordinates of secondary's vertices in plane xoy

Through recursion, all coordinates of a vertex can be derived from the first vertex. Take the primary coil as an example, we can put the coil at the same position as the secondary coil, and then use matrix transformation to derive the coordinates.

In Eq.(7), α, β and γ are the angles of rotation around the x, y and z axes and is positive in the counterclockwise direction. $[x_i, y_i, 0]$ is the coordi-

nates of the coil 2 at the beginning. $[x_0, y_0, z_0]$ is the translation vector, namely the coordinate of the center of n-polygon arbitrarily positioned in space. $[x_{k+1}, y_{k+1}, z_{k+1}]$ is the coordinate of n-polygon arbitrarily positioned in space. According to Eq.(4), we can calculate all the sides of n-polygon B_{zmag} and add B_{zmag} to derive B_{zmag} of the optional position produced by n-polygon.

$$\begin{bmatrix}\cos\gamma & -\sin\gamma & 0\\ \sin\gamma & \cos\gamma & 0\\ 0 & 0 & 1\end{bmatrix}\begin{bmatrix}\cos\beta & 0 & \sin\beta\\ 0 & 1 & 0\\ -\sin\beta & 0 & \cos\beta\end{bmatrix}\cdot \begin{bmatrix}1 & 0 & 0\\ 0 & \cos\alpha & -\sin\alpha\\ 0 & \sin\alpha & \cos\alpha\end{bmatrix}\begin{bmatrix}x_i\\ y_i\\ 0\end{bmatrix}+\begin{bmatrix}x_0\\ y_0\\ z_0\end{bmatrix}=\begin{bmatrix}x_i+1\\ y_i+1\\ z_i+1\end{bmatrix} \quad (7)$$

1.3 Numerical modeling of integral area

To deal with the division of integral area, as shown in Fig.4, this paper can take advantage of n-polygon's symmetry to divide the area into several isosceles trapezoids. Because we have known all the coordinates of the vertices according to Eq.(8), the integral area can be easily and explicitly expressed. According to symmetry, it only has to divide half of the integral area. Similarly, when odd polygons are involved, the integration area can be divided into several trapezoids, but the area is divided into more components to make the integration range easier to describe.

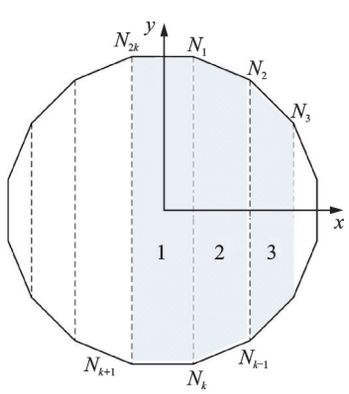

Fig.4 Division of n-polygon integral area

$$\begin{cases}\phi_1=\int_{X_{N_{2k}}}^{X_{N_1}}\int_{l_{N_{k+1}-N_k}}^{l_{N_{2k}-N_1}}(B_{1z}+B_{2z}+\cdots+B_{nz})\mathrm{d}x\mathrm{d}y\\ \phi_2=\int_{X_{N_1}}^{X_{N_2}}\int_{l_{N_k-N_{k-1}}}^{l_{N_2-N_1}}(B_{1z}+B_{2z}+\cdots+B_{nz})\mathrm{d}x\mathrm{d}y\\ \vdots\\ \phi_i=\int_{X_{N_{i-1}}}^{X_{N_i}}\int_{l_{N_{k+(2-i)}-N_{k+(1-i)}}}^{l_{N_{i-1}-N_i}}(B_{1z}+B_{2z}+\cdots+B_{nz})\mathrm{d}x\mathrm{d}y\end{cases} \quad (8)$$

where B_{1z}, B_{2z}, B_{nz} are the B_{zmag} produced by the first, the second and the n-th side. X_{N_i} is the x-coordinate of point N_i, and $l_{N_{i-1}-N_i}$ the equation of the line that goes through point N_{i-1} and point N_i. Because all the coordinates of the polygon are deduced above, the strip integral region can make it easier to describe the integration range

$$M=\frac{\phi_1+\phi_2+\cdots+\phi_i}{I} \quad (9)$$

The mutual inductance is obtained by adding up the magnetic flux generated by each edge.

2 Theoretical Simulation and Verification

2.1 Effect of displacement

To verify the calculation accuracy, we compare the calculation results with the results in Refs. [22-23]. In this paper, the comparison between theoretical calculation and simulation of coil mutual inductance is given. At different distances, the comparison results with octagon coils are shown in Fig.5.

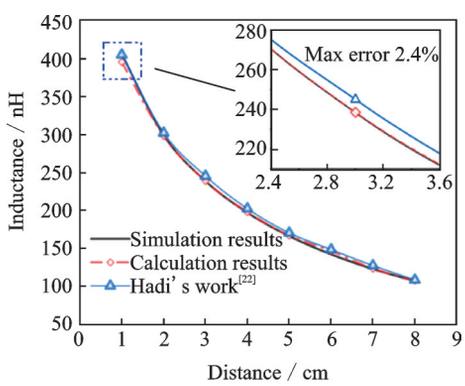

Fig.5 Comparison between simulation and theory results of mutual inductance of octagon coils

In the verification, we chose an octagonal coil with a side length of 10 cm and a current intensity of 1 A. The central coordinate of the secondary coil is $(0, 0, z)$. We make the two coils parallel. With the vertical distance between two coils as the independent variable, the following values are obtained with the help of Matlab software. At the same time, we used Ansoft Maxwell software for simulation. At different distances, the comparison results with Hexagon coils are shown in Fig.6

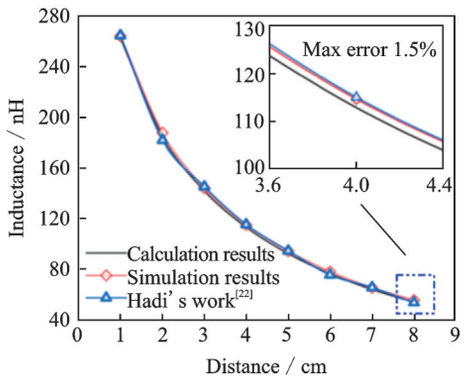

Fig.6 Comparison between simulation and theory results of mutual inductance of hexagon coils

Although the calculation results are different, our final data are consistent with the results of Hadi's formula. At the same time, the difference between our calculation and simulation is about 1.5%.

In this part, we compare the calculated results of the two groups with the results of Hadi's equation and Grover's formula. The calculation results of these two groups of hexagons and octagons are in good agreement with the simulation results, and the error rate is 2.8%. But in this case, only parallel motion is considered, and the experiment is not convincing enough.

2.2 Effects of rotation

Take rotation as a variable parameter for the next experiment. We use Ansoft Maxwell software for simulation, and use Matlab software to verify the calculation results. Taking the position of the second coil as the origin, the primary coil needs to rotate around the x-axis at an angle of α, around y-axis at β, and around z-axis at γ. We specify a positive counterclockwise direction.

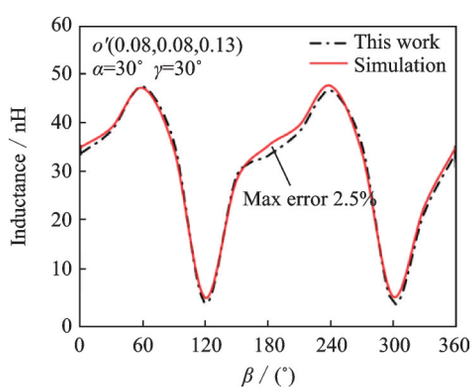

Fig.7 Comparison of octagon coils with different angles

In Fig.7, α is 30° and γ is 30°, and the central coordinate of the primary coil is (0.08, 0.08, 0.13). Take β as independent variable. Because the actual size of the coil is ignored in the calculation, there will still be an offset at some points, such as when β is 180° or 210°. The accuracy of the calculation method in this paper can be verified by comparing simulation with theoretical calculation.

For Section 1 and Section 2, the formula is verified from two aspects of parallel motion and rotation. We compared the calculation results with the results of two groups of Hadi equation and Grover formula, and our formula always matches their formula. In the rotation part, we conducted 13 groups of data comparison experiments. Through a large amount of data comparison, the maximum error rate is about 2.5% only when the rotation angle is 180°.

3 Experiments

In order to further verify the influence of angle between coils, we measure the mutual inductance of octagon coils using a precision 6-DOF platform and LCR tester, and the experimental diagram is shown in Fig.8.

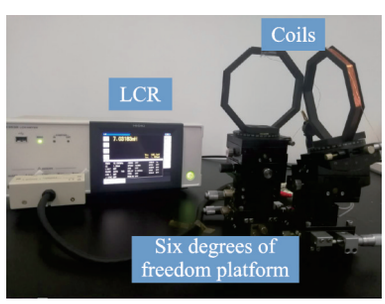

Fig.8 Experimental diagram

In the experiment, we use the same sized octagon coils with 180 turns, copper wire diameter 0.2 mm and the sides length 10 cm. The experimental measurement and theoretical calculation errors are shown in Fig.9.

When the central coordinate of the primary coil is (0.08, 0.08, 0.13), α is −20° and γ is −10°. Take β as our independent variable. The experimental measurement and theoretical calculation errors are shown in Fig.10.

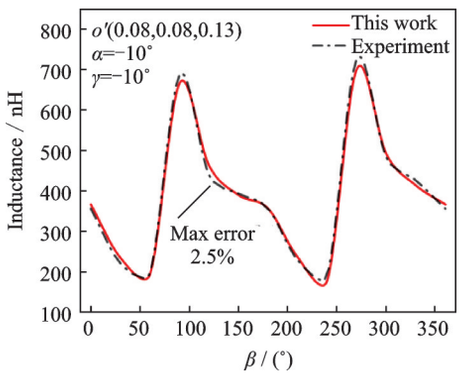

Fig.9 Comparison of calculational results with experimental measurement results ($\alpha=-10°$)

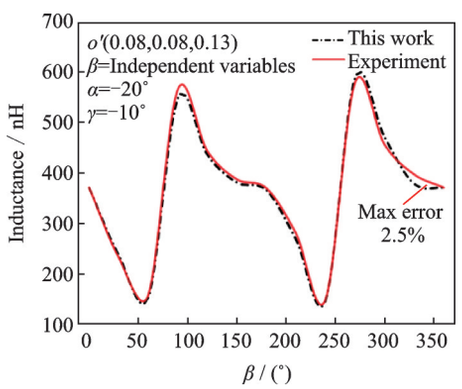

Fig.10 Comparison of calculational results with experimental measurement results ($\alpha=-20°$)

It can be seen that although the solutions are different, our final measured data are consistent with the simulation results. In the comparative experiment, from 26 groups of data, the error rate of few points exceeds 2.5%. In fact, the actual size and winding mode of the coil will also affect the measurement of mutual inductance, which cannot be ignored. But the difference between our measurement and simulation is about 1.5%. The experimental results show that the method of mutual inductance calculation is feasible.

4 Conclusions

A new calculation formula of regular polygon is proposed, which requires a vertex coordinate of secondary coil and a translation vector of primary coil. For octagonal coil, error between algorithm value and simulation value is 0.5%. In the actual experiment, the error ratio between experiment and simulation is about 1.5%. The new algorithm can simplify the procedure and enhance the accuracy of the calculation by updating the calculation of the objective function and the division of the feasible region.

References

[1] NI W, WANG X. Radio alignment for inductive charging of electric vehicles. Industrial Informatics[J]. IEEE Transactions on Industrial Informatics, 2015, 11(2): 427-440.

[2] LI S, MI C C. Wireless power transfer for electric vehicle applications[J]. IEEE Journal of Emerging and Selected Topics in Power Electronics, 2014, 3(1): 4-17.

[3] WU J, ZHAO C, LIN Z. Wireless power and data transfer via a common inductive link using frequency division multiplexing[J]. IEEE Transactions on Industrial Electronics, 2015, 62(12): 7810-7820.

[4] ZHANG Z, CHAU K T. An efficient wireless power transfer system with security considerations for electric vehicle applications[J]. Journal of Applied Physics, 2014, 115(17): 17A328.

[5] MOHAMED A A S, MARIM A A. Magnetic design considerations of bidirectional inductive wireless power transfer system for EV applications[J]. IEEE Transactions on Magnetics, 2017, 53(6): 1-5.

[6] CHA Y J, NAM B, KIM J. Evaluation of the planar inductive magnetic field sensors for metallic crack detections[J]. Sensors and Actuators A: Physical, 2010, 162(1): 13-19.

[7] HURLEY W G, DUFFY M C, ZHANG J. A unified approach to the calculation of self-and mutual-inductance for coaxial coils in air[J]. IEEE Transactions on Power Electronics, 2015, 30(11): 6155-6162.

[8] DE ANGELIS G, PASKU V. An indoor AC magnetic positioning system[J]. IEEE Transactions on Instrumentation and Measurement, 2014, 64(5): 1267-1275.

[9] PASKU V, DE ANGELIS A, DE ANGELIS G. Magnetic field-based positioning systems[J]. IEEE Communications Surveys & Tutorials, 2017, 19(3): 2003-2017.

[10] PASKU V, DE ANGELIS A, DIONOGI M. Analysis of nonideal effects and performance in magnetic positioning systems[J]. IEEE Transactions on Instrumentation and Measurement, 2016, 65(12): 2816-2827.

[11] PASKU V, DE ANGELIS A, DE ANGELIS G. Magnetic field analysis for 3-D positioning applications[J]. IEEE Transactions on Instrumentation and Measurement, 2017, 66(5): 935-943.

[12] GROVER F W. Formulas and tables for the calculation of the inductance of coils of polygonal form[M]. [S.l.]: US Government Printing Office, 1923.

[13] SU Y P, LIU X, HUI S Y R. Mutual inductance calculation of movable planar coils on parallel surfaces[J]. IEEE Transactions on Power Electronics,

2009, 24(4): 1115-1123.
[14] CHEN Y S, ZHU Z Q, HOWE D. Calculation of d- and q-axis inductances of PM brushless ac machines accounting for skew[J]. IEEE Transactions on Magnetics, 2005, 41(10): 3940-3942.
[15] AOMAR L, ALLAG H, FELIACHI M. 3-D integral approach for calculating mutual interactions between polygon-shaped massive coils[J]. IEEE Transactions on Magnetics, 2017, 53(11): 1-5.
[16] DEHUI W, QISHENG S, XIAOHONG W. Analytical model of mutual coupling between rectangular spiral coils with lateral misalignment for wireless power applications[J]. IET Power Electronics, 2018, 11(5): 781-786.
[17] DEHUI W, WANG X H. Analytical modeling and analysis of mutual inductance coupling of rectangular spiral coils in inductive power transfer[J]. Transactions of China Electrotechnical Society, 2018, 33(3): 680-688.
[18] DEHUI W, FAN Y, CHAO H. Method for the calculation of coupling coefficient between two arbitrar-shaped coils[J]. IET Power Electronics, 2019, 12(15): 3936-3941.
[19] BABIC S, SIROIS F, AKYEL C. Mutual inductance calculation between circular filaments arbitrarily positioned in space: Alternative to grover's formula[J]. IEEE transactions on magnetics, 2010, 46(9): 3591-3600.
[20] BABIC S, AKYEL C. Magnetic force between inclined circular filaments placed in any desired position[J]. IEEE transactions on magnetics, 2011, 48(1): 69-80.
[21] GROVER F W. Inductance calculations: Working formulas and tables[M]. [S.l.]: Courier Corporation, 2004.
[22] TAVAKKOLI H, ABBASPOUR E. Analytical study of mutual inductance of hexagonal and octagonal spiral planer coils[J]. Sensors and Actuators A: Physical, 2016, 247: 53-64.
[23] TAVAKKOLI H, ABBASPOUR E. Mutual inductance calculation between two coaxial planar spiral coils with an arbitrary number of sides[J]. Microelectronics Journal, 2019, 85: 98-108.

Authors Dr. **ZHANG Zijian** received the B.S. degree in mechanical engineering from Jinan University in 2008, the M.S. and Ph.D. degrees in mechatronic engineering from Harbin Institute of Technology in 2010 and 2016. His research is focused on magnetic sensor, robots and new aircraft.

Dr. **DONG Yangyang** received the B.S. degree in mathematics from Beihua University in 2008, the M.S. degree in probability theory and statistics from Harbin Institute of Technology in 2010 and Ph.D. degree in mechatronic engineering from Harbin Institute of Technology in 2016. Her research is focused on space robot technology and dynamics control.

Author contributions Dr. **ZHANG Zijian** provided the model and data for analysis. Dr. **SHAO Ming** designed the research and contributed to the discussion and revision of the manuscript. Mr. **SHANG Kai** finished the simulation and experiments. Mr. **LI Xuekong**, Mr. **HUANG Chunliang**, Mr. **SHI Jinku**, and Mr. **CUI Huaxian** provided experimental equipment and assisted in coil mutual inductance measurement experiments and data processing. Dr. **DONG Yangyang** was responsible for writing and proofreading papers. All authors commented on the manuscript draft and approved the submission.

Competing interests The authors declare no competing interests.

(Production Editor: SUN Jing)

任意位姿下多边形线圈间互感的计算

张子建[1],邵　明[1,2],尚　恺[3],李学孔[4],黄纯亮[4],石金库[4],
崔华先[4],董洋洋[1]

(1.南京航空航天大学航天学院,南京 210016,中国;2.上海航天技术研究院第804研究所,上海 201100,中国;
3.中国航天科工集团第41研究所,呼和浩特 010010,中国;4.华能广西能源有限公司,南宁 530028,中国)

摘要:多边形线圈系统是针对种类越来越多的传感器和电磁系统而设计的。本文提出了一种包括不规则多边形在内的多边形线圈之间的互感计算方法。该方法基于毕奥-萨伐尔定律,通过将多边形线圈分割成有限长的线来计算互感,将激励线圈产生的磁感应强度表达为关于线圈各个顶点空间位置的函数。更新了目标函数可行域的计算方式并简化了计算过程,从而提高了计算精度并通过仿真和实验验证了该算法的准确性。

关键词:互感;多边形线圈;毕奥萨伐尔定律;任意位姿